Electronic Supplementary Material (ESI) for Nanoscale.

Electronic Supplementary Information

Boron-Nitrogen Substituted Planar Core: A Strategy in Designing Dopant-Free Hole-transporting Materials for Efficient Perovskite Solar Cells

Mengyao Hao [a], Weijie Chi [b], Zesheng Li [a*]*

[a] Key Laboratory of Cluster Science of Ministry of Education, Beijing Key Laboratory of Photoelectronic/Electrophotonic Conversion Materials, School of Chemistry and Chemical Engineering, Beijing Institute of Technology, Beijing 100081, China

[b] Fluorescence Research Group, Singapore University of Technology and Design, 8 Somapah Road, 487372 Singapore

Corresponding authors

E-mail: weijie_chi@sutd.edu.sg

E-mail: zeshengli@bit.edu.cn

Contents

Computational details

For isolated molecular properties, the geometries of all investigated single molecules are relaxed to their potential energy minimum at the B3LYP/6-31G(d, p) level in dichloromethane solvent, based on the conductor-like polarizable continuum model (C-PCM).[1] Time-dependent density functional theory (TD-DFT) calculation was also carried out to simulate the photochemical properties and excite state of HTMs based on M06-2X/6-31G(d, p) level. All calculations are performed using Gaussian 16 code.[2] Molecule stable dimers are obtained through two steps. Firstly, MD of 30 ps simulation are carried out at 298K in the NVE ensemble with a time step of 1 fs by using the DFTB+ 1.0.1 package to get tough dimeric structures. Secondly, the rough dimers with the lowest energies from dynamics simulation are selected as the starting geometries and optimized to their potential energy minimum at B3LYP/6-31G(d, p) level with Gaussian 16 program package.

The hole mobility of the investigated molecules is calculated by using the Einstein relation:[3]

$$\mu = \frac{e r^2}{2 k_B T} k$$

where *e* is the charge. *r* denotes the distance between two mass centers.

The Marcus theory with the hopping model is employed to describe the hole transport behavior. The charge hopping rate (*k*) is expressed as:[4]

$$k = \frac{4\pi^2}{h} v^2 \frac{1}{\sqrt{4\pi k_B T}} \exp\left[- \frac{\lambda}{4 k_B T} \right]$$

where k_B represents the Boltzmann constant, *T* is the temperature in Kelvin, and *h* denotes the Planck constant. *λ* represents the reorganization energy, which is calculated by using the adiabatic potential energy surface method. In this work, only internal reorganization energy is considered. The reorganization energy can be expressed as follows:[5]

$$\lambda = (E_0^* - E_0) + (E_+^* - E_+)$$

where E_+^* and E_0^* represent the total energies of cationic and neutral species with the geometries of the neutral and cationic species, respectively. E_+ and E_0 are the total

energies of the cationic and neutral molecules in their lowest energy geometries, respectively.

v denotes the transfer integral, which is obtained by adopting a direct approach at the M06-2X/6-31G(d, p) level. In our work, *v* can be written as:[6]

$$v = \langle \psi^{HOMO}_{i} | F | \psi^{HOMO}_{f} \rangle$$

where ψ^{HOMO}_{i} and ψ^{HOMO}_{f} represent the HOMOs of the isolated molecules 1 and 2. *F* is the Fock operator for the dimer, which can be calculated as: $F=SC\varepsilon C^{-1}$

The Kohn-Sham Orbital *C* and eigenvalue ε are evaluated by diagonalizing the zeroth-order Fock matrix. *S* denotes the overlap matrix for the dimer.

For HTMs-$CH_3NH_3PbI_3$ interfacial properties, the geometry optimization were calculated by the generalized gradient approximation (GGA) parametrized with Perdew-Burke Ernzerhof (PBE) and the related properties were all used by Vienna Ab Initio Simulation Package (VASP).[7-9]

The plane wave energy cutoff is set to 500 eV with the application of periodic boundary conditions for the structures of HTM molecule and $CH_3NH_3PbI_3$ (797 atoms), and all atomic positions are fully relaxed during optimization (residual forces, <0.01 eV/Å). The k-point grids of 1 × 1 × 1 and 2 × 2 × 1 are adopted for geometry optimization and electronic properties calculations, respectively. Van der Waals (vdW) interactions are considered with Grimme's DFT-D3 correction to describe weak interactions between the HTM molecule and $CH_3NH_3PbI_3$.[10] Spin-orbit coupling (SOC) is a spin-dependent relativistic correction to the Born-Oppenheimer Hamiltonian and is more prominent for heavy elements such as Pb.[11] SOC is taken into account combined with the PBE exchange-correlation functional. The electronic properties are calculated by using the hybrid PBE0 functional.[12] The optical properties are obtained from the dielectric function $\varepsilon(\omega)$ and absorption spectra $A(\omega)$, which can be determined from the corresponding electronic structures.[13]

Table S1 Calculated oscillator strength f, maximum wavelengths λ_{abs}(nm), transition energy E_g(eV) of absorption and maximum wavelengths λ_{em}(nm)， transition energy E_1(eV) of emission and Stokes shifts.

Molecules	Absorption				Emission		Stokes Shifts
	f	λ_{abs}	E_g	Major configuration	λ_{em}	E_1	
BN-TTN-B1	1.36	367.7	3.37	HOMO > LUMO (76%)	465.4	2.66	97.7
BN-TTN-N1	1.35	377.8	3.28	HOMO > LUMO (82%)	483.2	2.57	105.4
BN-TTN-B2	2.07	372.5	3.33	HOMO > LUMO (63%) HOMO-1 > LUMO+1(19%)	465.8	2.66	93.3
BN-TTN-N2	2.38	384.3	3.23	HOMO > LUMO (48%) HOMO-1 > LUMO+1(37%)	483.4	2.56	99.1
BN-TTN-BN1	1.96	376.4	3.29	HOMO-1 > LUMO (43%) HOMO > LUMO (24%)	484.3	2.56	107.9
BN-TTN-BN2	1.96	411.9	3.01	HOMO > LUMO (82%)	525.4	2.36	113.5
BN-TTN-B3	1.91	409.2	3.03	HOMO > LUMO (75%)	525.6	2.36	116.4
BN-TTN-N3	1.85	408.5	3.04	HOMO-1 > LUMO+1(61%) HOMO > LUMO+1(12%)	525.1	2.36	116.6
BN-TTN-4	3.63	406.5	3.05	HOMO > LUMO (58%) HOMO-1 > LUMO+1(23%)	525.7	2.36	119.2
Spiro-OMeTAD	1.22	346.2	3.58	HOMO-1 > LUMO (51%) HOMO > LUMO (42%)	410.2	3.02	64.0

Table S2 The adiabatic ionization potentials (IP_a, eV), adiabatic electron affinities (EA_a, eV), the absolute hardness (η), hydrophobic property (Log$P$) and solvation free energy (ΔG_{solv}, kcal/mol) calculated at the B3LYP/6-31G** level.

Molecules	IPa	EAa	η	Log$P$ (octanol/water)	Log$P$ (dichloromethane/water)	ΔG_{solv}
BN-TTN-B1	4.63	1.61	1.51	8.17	14.97	-30.61
BN-TTN-N1	4.68	1.66	1.51	8.20	15.00	-30.37
BN-TTN-B2	4.62	1.66	1.48	11.97	22.19	-46.04
BN-TTN-N2	4.66	1.65	1.50	11.98	22.22	-45.83
BN-TTN-BN1	4.61	1.67	1.47	11.99	22.22	-45.99
BN-TTN-BN2	4.51	1.78	1.36	11.96	22.19	-46.03
BN-TTN-B3	4.49	1.77	1.36	15.76	29.42	-61.56
BN-TTN-N3	4.49	1.76	1.37	15.72	29.14	-61.46
BN-TTN-4	4.46	1.79	1.34	19.52	36.61	-77.12
Spiro-OMeTAD	4.42	1.21	1.61	14.16	27.06	-59.24

Table S3 the changes of dihedral angles in BN-TTN core and triphenylamines from neutral to cationic molecule.

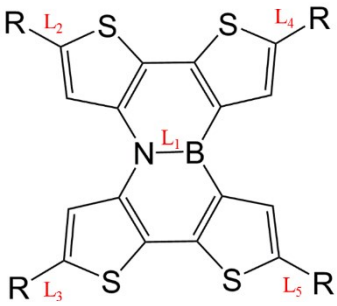

molecules	Φ_1		Φ_2		Φ_3		Φ_4		Φ_5	
	Neutral	Cation	Neutral	Cation	Neutral	Cation	Neutral	Cation	Neutral	Cation
BN-TTN-B1	164.92	164.01	156.80	171.48	\	\	\	\	\	\
BN-TTN-N1	165.22	164.38	\	\	157.15	170.08	\	\	\	\
BN-TTN-B2	165.16	164.17	156.76	173.38	\	\	\	\	156.76	157.98
BN-TTN-N2	165.52	165.32	\	\	156.81	171.36	156.15	158.58	\	\
BN-TTN-BN1	165.40	164.15	155.82	173.33	\	\	155.15	158.97	\	\
BN-TTN-BN2	165.36	163.82	158.94	171.20	160.08	168.51	\	\	\	\
BN-TTN-B3	165.38	163.87	158.49	173.19	156.16	169.68	\	\	155.45	156.50
BN-TTN-N3	165.08	163.75	159.27	171.29	154.87	170.30	157.75	158.91	\	\
BN-TTN-4	165.15	164.34	156.67	177.49	160.79	177.63	157.17	160.84	157.20	159.96

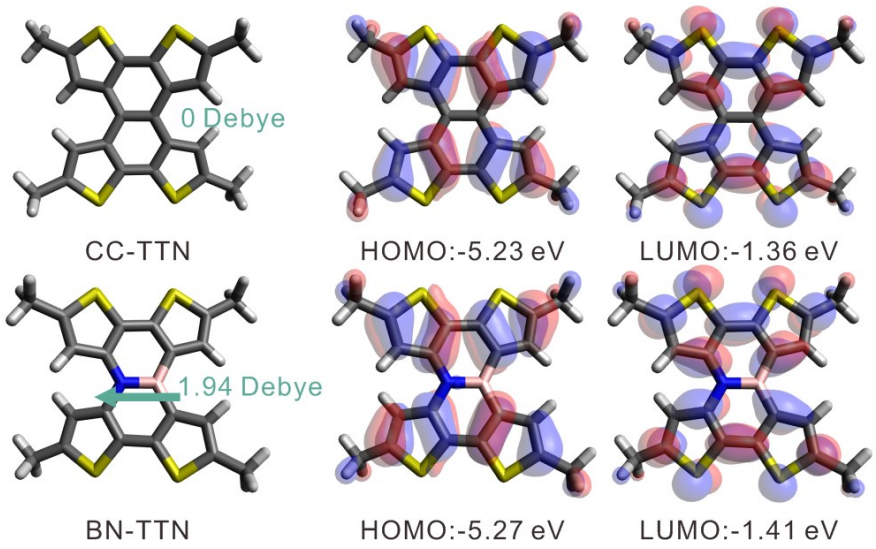

Figure S1 Energy level diagram for CC-TTN and BN-TTN. The HOMO and LUMO values of two molecules are computed by the B3LYP/6-31G** level.

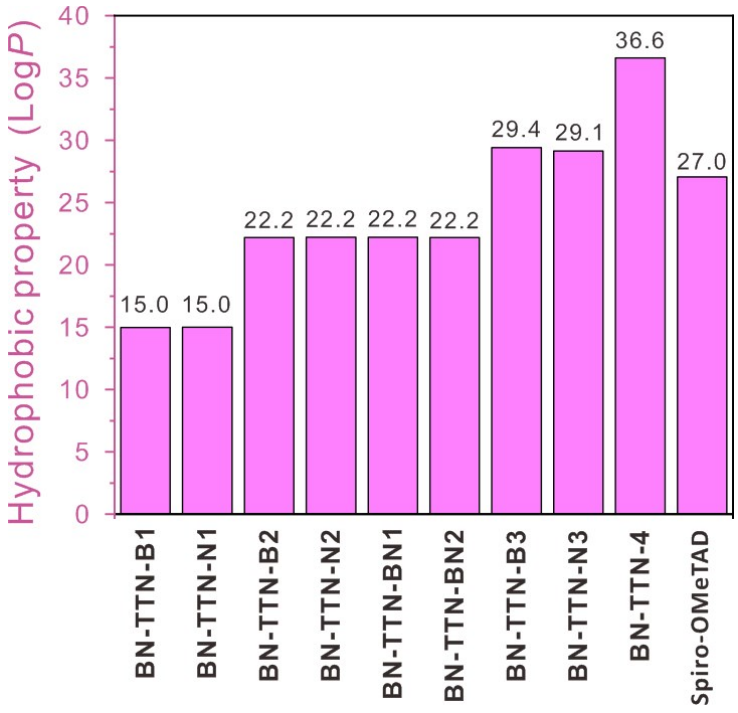

Figure S2 The changing trend of hydrophobic property (Log*P*) in the dichloromethane solvent from **BN-TTN-B1** to **BN-TTN-4** along with Spiro-OMeTAD.

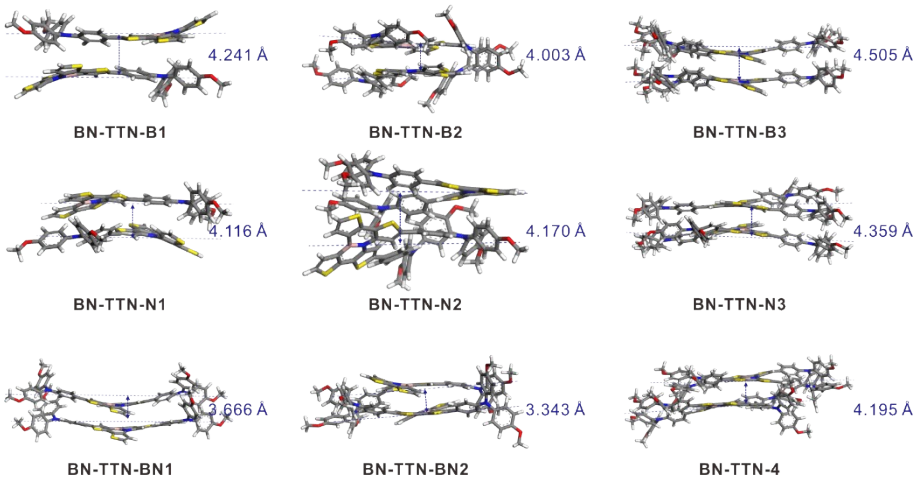

Figure S3 The optimized structure (side view) of all target molecules. Among them, the plane distances of the neighboring molecules are shown in blue.

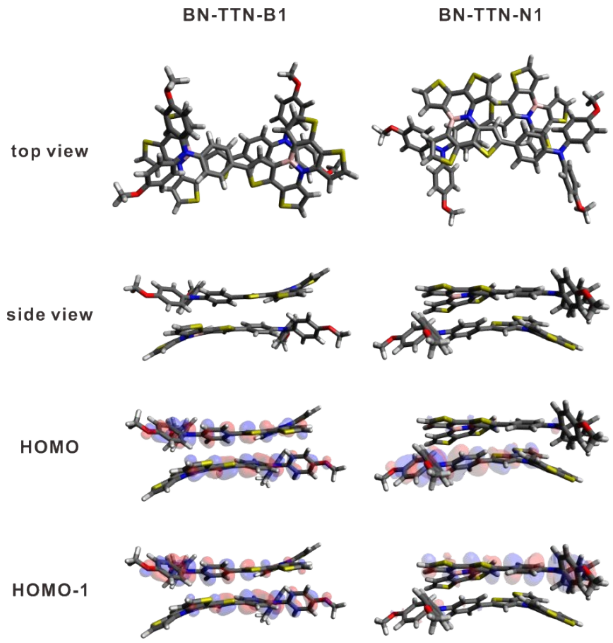

Figure S4 The optimized structure (top view and side view), orbital distributions of **BN-TTN-B1** and **BN-TTN-N1** dimer.

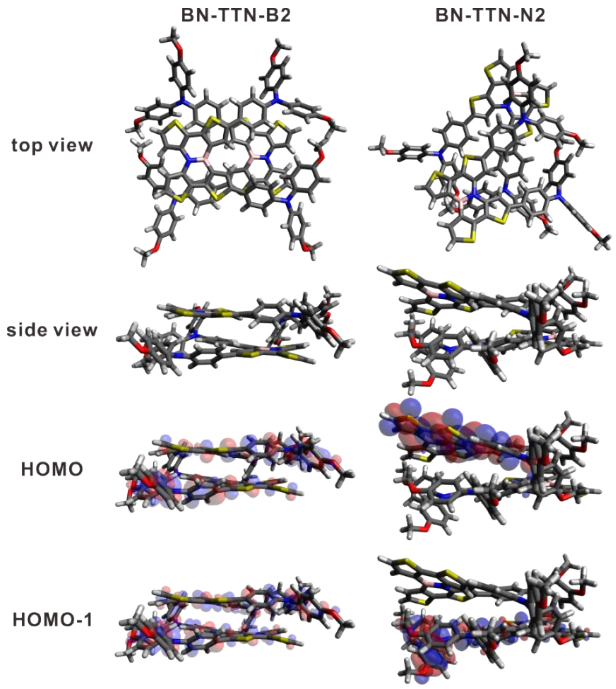

Figure S5 The optimized structure (top view and side view), orbital distributions of **BN-TTN-B2** and **BN-TTN-N2** dimer.

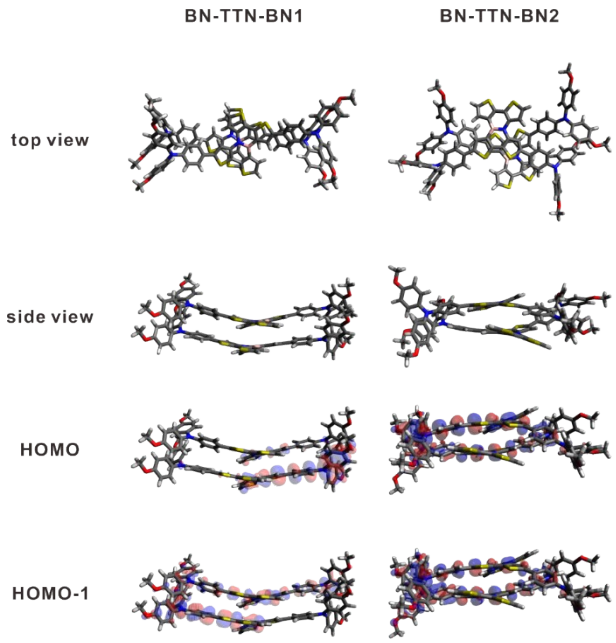

Figure S6 The optimized structure (top view and side view), orbital distributions of **BN-TTN-BN1** and **BN-TTN-BN2** dimer.

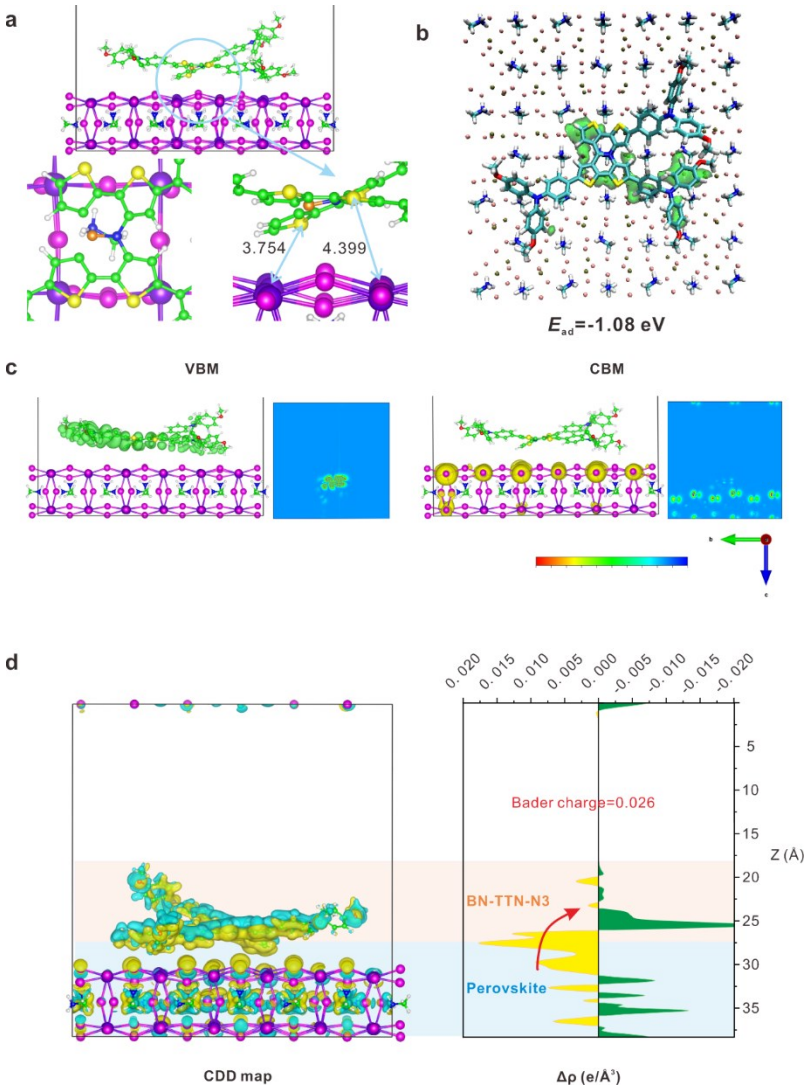

Figure S7 a) the front and top views of the optimized structure for **BN-TTN-N3**/perovskite (lie one), And the S-Pb bond length along with the surface binding energy are shown. **b)** the independent gradient model (IGM) to perform a detailed analysis of the interaction between HTM and perovskite for **BN-TTN-N3**. Green represents the area of weak interaction. **c)** the contour plots of the CBM, and VBM, along with the electrostatic potentials of the CBM and VBM viewed from the (010) surface. **d)** Isosurface view of spatial charge density difference at the same value upon the formation of the HTM/perovskite interface; the yellow and cyan color indicate the electron gain and loss, respectively. And the planar average electron density difference ($\Delta\rho$) integrated over the x−y plane for the HTM/perovskite systems as a function of the z coordinate (perpendicular to the surface).

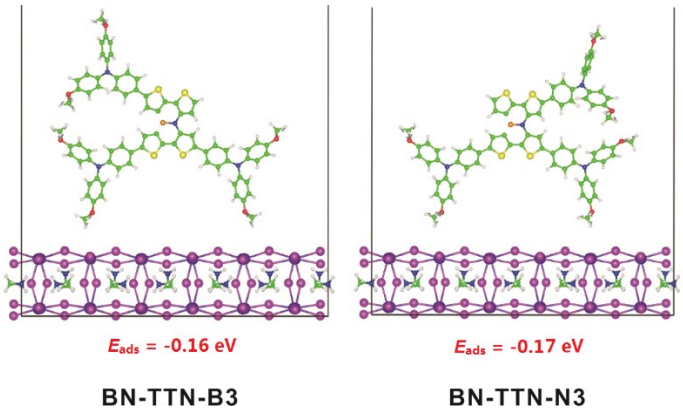

Figure S8 the optimized structure (stand one) and the surface binding energy for **BN-TTN-B3** and **BN-TTN-N3**, respectively.

References

1. A. V. Marenich, C. J. Cramer and D. G. Truhlar, *J Phys Chem B*, 2009, **113**, 6378-6396.
2. M. Frisch, G. Trucks, H. Schlegel, G. Scuseria, M. Robb, J. Cheeseman, G. Scalmani, V. Barone, G. Petersson and H. Nakatsuji, Gaussian, Inc. *Wallingford,* CT, 2016.
3. J. Cornil, V. Lemaur, J.-P. Calbert and J.-L. Brédas, *Adv. Mater.*, 2002, **14**, 726-729.
4. R. A. Marcus, *Angew. Chem. Int. Ed.*, 1993, **32**, 1 1 1 1 - 1222.
5. G. Nan, L. Wang, X. Yang, Z. Shuai and Y. Zhao, *J Chem Phys*, 2009, **130**, 024704.
6. W. Linjun, N. Guangjun, Y. Xiaodi, P. Qian, L. Qikai and S. Zhigang, *Chem. Soc. Rev.*, 2010, **39**, 423-434.
7. G. Kresse and D. Joubert, *Phys. Rev. B*, 1999, **59**, 1758-1775.
8. G. Kresse and J. Furthmüller, *Phys. Rev. B*, 1996, **54**, 11169-11186.
9. Y. Zhou, W. Yu, A. Khan, X. Chong and J. Feng, *J Micro Mol Phys*, 2020, **05**, 2030001.
10. S. Grimme, J. Antony, S. Ehrlich and H. Krieg, *J. Chem. Phys.*, 2010, **132**, 154104.
11. J. Even, L. Pedesseau, J.-M. Jancu and C. Katan, *J Phys Chem Lett*, 2013, **4**, 2999-3005.
12. C. S. Adamo, G. E.; Barone, V., *J. Chem. Phys.*, 1999, **111**, 2889-2899.
13. P.-P. Sun, Q.-S. Li, L.-N. Yang and Z.-S. Li, *Nanoscale*, 2016, **8**, 1503-1512.